Optical Polarization Modulation and Gain Anisotropy in an Electrically Injected Spin Laser

D. Basu, D. Saha, and P. Bhattacharya*

Solid-State Electronics Laboratory, Department of Electrical Engineering and Computer Science, University of Michigan, 1301 Beal Avenue, Ann Arbor, Michigan 48109-2122, USA

(Received 1 July 2008; published 5 March 2009)

The effects of spin-induced gain anisotropy on output polarization and threshold current reduction of electrically pumped spin-polarized lasers have been studied. Analytical forms of these parameters are derived by considering diffusive transport from the spin injector to the active region. The calculated values of the parameter are in excellent agreement with values obtained from measurements made at 200 K on an InAs/GaAs quantum dot spin-polarized vertical cavity surface-emitting laser. Electrical modulation of the output polarization of the laser is demonstrated with a peak modulation index of 0.6.

DOI: 10.1103/PhysRevLett.102.093904 PACS numbers: 42.55.Px, 72.25.Hg, 72.25.Mk, 72.25.Pn

The ability to dynamically switch between orthogonal polarization states in spin-polarized semiconductor lasers with the bias current, which are otherwise difficult to predict, stabilize, or control [1–3], offers a novel and elegant technique for secure communication in a lightwave network. Other envisaged applications include reconfigurable optical interconnects, the study of vitamins, and asymmetric photochemical synthesis [4]. Spin-polarized lasers also promise reduced threshold current [5,6], enhanced emission intensity, and optical communication with enhanced bandwidth [7].

In electrically pumped spin-polarized light sources, a nonequilibrium spin population is injected from a magnetic contact to the forward biased active region of a diode consisting of nonmagnetic semiconductors [8]. The active region can be a bulk semiconductor or quantum structures such as quantum wells, wires, or dots [9]. The selection rules for the conservation of angular momentum directly relate the spin orientation of the carriers transported to the active region to the polarization of photons emitted upon their radiative recombination [10]. While these relations hold for spontaneous emission, such as in a spin light emitting diode, they do not reflect the output polarization in a spin laser [5] due to the nonlinear dynamics and the spin polarization in the gain medium (active region), which gives rise to a large gain anisotropy at biases near threshold. As a result, the output polarization can be much larger than the spin polarization of the injected carriers. This has been observed by us in quantum well spin lasers [6], but the exact magnitude of the output polarization and the parameters and dynamics upon which it depends have been hitherto unknown. In the present study, we have derived the analytical form of the output polarization Π_c, the threshold current $I_{\mathrm{th}}(H)$, and the threshold current reduction $\Delta I_{\mathrm{th}}/I_{\mathrm{th},0}$, as determined by gain anisotropy. In particular, we have highlighted the role of the diffusive transport of spin-polarized electrons from the ferromagnetic contact to the active region. The calculated values of these parameters are in excellent agreement with values obtained from the first measurement of electrical modulation of a InAs/GaAs quantum dot (QD) spin-polarized vertical cavity surface-emitting laser (VCSEL) with MnAs ferromagnetic contacts, schematically shown in Fig. 1(a). The quantum dot active region allows high temperature operation since the spin relaxation time in the dots, limited by the D'yakonov-Perel spin scattering process [11], is enhanced due to carrier confinement. The present study provides a comprehensive insight to the operation and characteristics of an electrically injected spin-polarized semiconductor laser.

An important aspect which has to be taken into account in any spin laser, edge- or surface-emitting, is the diffusive spin transport from the ferromagnetic contact to the active region. Spin polarization at a distance x from the ferromagnetic contact at $x = 0$ [see Fig. 1(b)] is governed by [12]

$$\frac{\partial^2(N^+ - N^-)}{\partial x^2} = \frac{N^+ - N^-}{\lambda_{\mathrm{sf}}^2}, \tag{1}$$

where λ_{sf} is the spin diffusion length in the transport medium and $N^+(x)$ and $N^-(x)$ are the spin-up and spin-down carrier densities, respectively, at any point x. Drift of

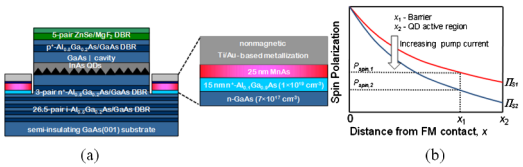

FIG. 1 (color online). (a) Heterostructure of a GaAs-based spin VCSEL grown by molecular beam epitaxy. The active (gain) region consists of InAs/GaAs quantum dots placed in a GaAs λ cavity. The ferromagnetic $MnAs/Al_{0.1}Ga_{0.9}As$ tunnel injector contact is regrown selectively on GaAs, as shown in the figure. (b) Schematic representation of the variation of carrier spin polarization with distance from ferromagnetic contact (MnAs) in a VCSEL in accordance with the spin diffusion equation. The barrier (cavity) is at distance x_1, and the quantum dot region is at distance x_2. In the barrier and quantum dots, the polarization decreases from $P_{\mathrm{spin},1}$ to $P_{\mathrm{spin},2}$ and Π_{S1} to Π_{S2}, respectively.

spin-polarized carriers is neglected since the doping densities in the transport region are relatively high ($\sim 5 \times 10^{17}$ cm^{-3}). These functions are valid from the contact up to the barrier (cavity) region, i.e., $x = x_1$. For $x > x_1$, the polarization is governed by the laser parameters. Also, we know that the ferromagnetic contact polarization is given by

$$P_{\text{contact}} = \Pi(x = 0) = \frac{N^+(x = 0) - N^-(x = 0)}{N^+(x = 0) + N^-(x = 0)}. \quad (2)$$

The value of P_{contact} is known from a measurement of the out-of-plane magnetization of the MnAs contact as a function of H [13], the spin-dependent density of states of MnAs [14], and the spin injection efficiency at the MnAs/GaAs tunnel barrier [15].

The dynamics of carrier and photon densities in semiconductor lasers are governed by the coupled rate equations as outlined in Refs. [5,16]. The parameters used in the model along with the values for our laser are listed in Table I. The nonlinear gain in the active region is generally expressed in terms of the gain compression factor ϵ as $g(n, S) = dg/dn\ (n - n_{\text{tr}})/(1 + \epsilon S)$, where $n(= n^+ + n^-)$ is the total (sum of spin-up and spin-down electrons) carrier density in the active region. Since the laser is operated very close to threshold where the gain anisotropy is a maximum, $\epsilon S \ll 1$, and hence $g(n, S) \cong g(n)$.

The laser rate equations and the spin diffusion equation are solved with the objective of obtaining analytical forms of the threshold current (and hence the threshold current reduction) and output polarization as a function of applied magnetic field. In solving these equations, we define a set of intermediate parameters. These are the spin polarization at any point $x(0 \le x \le x_1)$, $\Pi(x)$, the quantum dot spin polarization $\Pi_s = (n^+ - n^-)/(n^+ - n^-)$, and the average barrier polarization $\Pi_{s,b} = ({n_b}^+ - {n_b}^-)/({n_b}^+ - {n_b}^-)$, where $n_b^{\pm}$ is the spin-up (spin-down) carrier density at the barrier. On the other hand, the degree of circular polarization of the output $\Pi_c = (S^+ - S^-)/(S^+ + S^-)$ and the light output $L = S^+ + S^-$ are measurable quantities, where $S^{\pm}$ are the density of the right- and left-circularly polarized photons, respectively. By solving the steady state laser rate equations [17] it can be easily shown that the barrier polarization and the output circular polarization are related to the carrier density through

TABLE I. Spin laser model parameters and their values for a InAs/GaAs QD spin VCSEL at 200 K.

Parameter	Symbol	Value
Differential gain	dg/dn	3.4×10^{-14} cm^2
Rad. recombination coeff.	B_{sp}	9.4×10^{-19} cm^3 s^{-1}
Auger recombination coeff.	C	1.5×10^{-27} cm^6 s^{-1}
Carrier capture time	τ_{cap}	45 ps
Spin-flip time in barrier	$\tau_{s,b}$	300 ps
Spin-flip time in QD	τ_s	150 ps
Photon group velocity	v_g	8.7×10^9 cm s^{-1}
Optical confinement factor	Γ	0.024
Spontaneous emission factor	β	6×10^{-4}
Photon lifetime	τ_{ph}	1 ps
Threshold carrier density	n_{th}	4.66×10^{18} cm^{-3}
Transparency carrier density	n_{tr}	4×10^{17} cm^{-3}
Ferromagnetic contact polarization	P_{contact}	0.31
Spin diffusion length	λ_{sf}	0.6×10^{-4} cm
Barrier volume	V_b	2.1×10^{-11} cm^3
Active region volume	V_{QD}	2.8×10^{-13} cm^3

$$\frac{V_b}{V_{\text{QD}}}\frac{n_b}{\tau_{\text{cap}}} = v_g[g(n^+)S^- + g(n^-)S^+] + B_{\text{sp}}n^2 + Cn^3, \quad (3)$$

$$\frac{V_b}{V_{\text{QD}}}\frac{n_b^+ - n_b^-}{\tau_{\text{cap}}} = v_g[g(n^+)S^- - g(n^-)S^+] + (n^+ - n^-)\left(B_{\text{sp}}n + Cn^2 + \frac{2}{\tau_s}\right). \quad (4)$$

Similarly, the output circular polarization is related to the carrier density through

$$v_g[g(n^+)S^- + g(n^-)S^+] = \frac{S}{\Gamma\tau_{\text{ph}}} - \beta B_{\text{sp}}n^2, \quad (5)$$

$$v_g[g(n^+)S^- - g(n^-)S^+] = -\frac{S^+ - S^-}{\Gamma\tau_{\text{ph}}} - \beta B_{\text{sp}}n(n^+ - n^-), \quad (6)$$

where $S^{\pm}$ are given by

$$S^{\pm} = \frac{\Gamma\beta B_{\text{sp}}n^{\mp}n}{1/\tau_{\text{ph}} - \Gamma v_g g(n^{\mp})}. \quad (7)$$

Combining Eqs. (3) and (5), and noting that the pump current $I_{\text{pump}} = I_{\text{th}}$ when $n = n_{\text{th}}/(1 + \Pi_s)$, we get

$$I_{\text{th}}(H) = qV_{\text{QD}}\left[\frac{1}{\Gamma}\frac{S_{\text{th}}}{\tau_{\text{ph}}} + \frac{B_{\text{sp}}n_{\text{th}}^2(1 - \beta)}{[1 + \Pi_s(H)]^2} + \frac{Cn_{\text{th}}^3}{[1 + \Pi_s(H)]^3}\right], \quad (8)$$

where S_{th} is the photon density at threshold. It is found that the cumulative contribution from the terms containing the threshold photon density (S_{th}) and the Auger recombination coefficient (C) in Eq. (8) is less than 10% of the contribution from the term having the radiative recombination coefficient (B_{sp}), under all possible operating conditions of a spin laser. Hence, knowing $I_{\text{th},0}$, the percentage threshold current reduction $\Delta I_{\text{th}}(H)/I_{\text{th},0}$ is reduced to a simplified form given by

$$\frac{\Delta I_{\text{th}}(H)}{I_{\text{th},0}} \cong \frac{\Pi_s(\Pi_s + 2)}{(1 + \Pi_s)^2}. \quad (9)$$

It is of interest to note that this parameter is determined exclusively by Π_S. Therefore, parameters such as gain and

differential gain of the active material or the quality factor of the laser cavity will not play a role in determining percentage threshold current reduction.

Similarly, the output polarization [as obtained by using Eq. (7) and Eqs. (5) and (6)] is given by

$$\frac{\Pi_c(H, I_{\text{pump}})}{\Pi_s} = -\frac{1 + \Gamma v_g \tau_{\text{ph}} \frac{dg}{dn} n_{\text{tr}}}{1 + \Gamma v_g \tau_{\text{ph}} \frac{dg}{dn} n_{\text{tr}} - \Gamma v_g \tau_{\text{ph}} \frac{dg}{dn} n_{\text{th}}(1 - \Pi_s)}. \quad (10)$$

We also define a gain anisotropy parameter:

$$g_A(H, I_{\text{pump}}) = \frac{g(n^+)}{g(n^-)} \cong \frac{1 + \Pi_s}{1 - \Pi_s}. \quad (11)$$

The parameters $(\Delta I_{\text{th}}/I_{\text{th},0})$, g_A, Π_c, and $d\Pi_c/d(I_{\text{th}}/I_{\text{th},0})$ are plotted against the injection current and applied magnetic field and are depicted in Figs. 2 and 3. The device and material parameters used and obtained from our own work and from recent reports [18–21] are listed in Table I. The calculated data will be discussed in detail along with the experimental results to be presented next.

Measurements have been carried out on spin-polarized quantum dot VCSELs [Fig. 1(a)] grown by molecular beam epitaxy. The active region is comprised of 10 layers of InAs quantum dots. Circular post devices with mesa diameters from 15 to 30 μm diameter were fabricated by standard processing techniques [13]. As illustrated in Fig. 1(a), a MnAs (25 nm)/n^+-$Al_{0.1}Ga_{0.9}As$ (15 nm) Schottky barrier heterostructure is selectively regrown after a mesa definition, to form the spin polarized electron injector contact [22] and is critical in the context of electron spin injection [23]. We have earlier measured the injected spin polarization at identical MnAs tunnel injectors to be 31% [15]. Identical control VCSELs were also fabricated with a Ti/Au nonmagnetic contact replacing the MnAs injector.

The lasers were mounted in a magneto-optical cryostat for measurements, which were done in the Faraday geometry. All measurements reported here were carried out on 15 μm diameter VCSELs at the design temperature of 200 K where no offset exists between the photoluminescence gain peak and the distributed Bragg reflector (DBR) reflectivity peak, and hence lasing with the minimum threshold current is obtained. This temperature is carefully chosen such that a large number of spin-polarized carriers can still reach the QD active region. The current biasing to the lasers was in the continuous wave mode. The measured reduction and percentage reduction $(\Delta I_{\text{th}}/I_{\text{th},0})$ of the threshold current with the application of magnetic field are plotted in Fig. 2(a) and its inset, and there is good agreement with the calculated values of the respective parameters. A maximum threshold current reduction $(\Delta I_{\text{th}}/I_{\text{th},0})$ of ~8% is measured at $H = 2.1$ T, at which field the saturation of the out-of-plane magnetization of MnAs contact also occurs. No threshold reduction is observed for the nonmagnetic VCSEL. The calculated variation of gain anisotropy with current [Fig. 2(b)] indicates that spin-related phenomena are operative only for lasers biased near threshold $I_{\text{th},0}$. It may be noted that the gain anisotropy (g_A) is largest just below threshold. This is easily understood by considering injection of spin-polarized carriers in a laser biased slightly below threshold $I_{\text{th},0}$. An application of magnetic field results in injection of spin-polarized carriers which can preferentially enhance the gain of one polarization mode above threshold gain, while the gain of the other polarization mode still remains

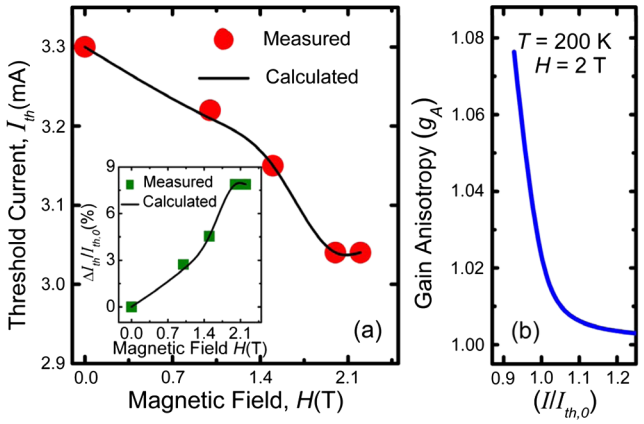

FIG. 2 (color online). Data from a 15 μm diameter InAs/GaAs QD spin VCSEL at 200 K: (a) calculated and measured reduction of threshold current with magnetic field applied perpendicular (hard axis) to the plane of the MnAs contact. The inset shows the calculated and measured percentage reduction of threshold current with field; (b) calculated variation of the gain anisotropy parameter, as defined in Eq. (9) (text) with normalized pump current.

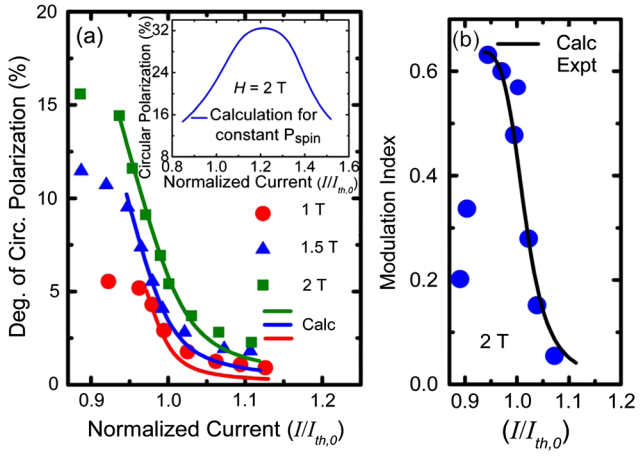

FIG. 3 (color online). (a) Calculated and measured modulation of output circular polarization of a InAs/GaAs QD spin VCSEL as a function of normalized pump current at different magnetic fields. The inset shows calculated polarization for constant pump current spin polarization, instead of the variation of P_{spin} shown in Fig. 1(b); (b) measured modulation index versus pump current. The calculated values are shown for currents at and above threshold.

subthreshold, resulting in a large gain anisotropy and reduction in the threshold current. As the injection is increased, the difference in peak gain of the two polarization modes will decrease, and the gain anisotropy will also steadily decrease. Needless to say, it is desirable to have the highest possible value of g_A. The maximum value of g_A attainable with a ferromagnetic MnAs spin injector is ~ 2, under the ideal conditions of negligible spin flip during transport of spin-polarized carriers to the active region. An increase in spin injection efficiency will lead to higher gain anisotropy [Eq. (11)] and hence enhanced threshold reduction and output circular polarization.

The output polarization characteristics of the spin laser are discussed next. For a fixed bias current, the measured value of Π_c as a function of the applied magnetic field follows the measured out-of-plane magnetization of the MnAs contact very closely. In comparison, the observed polarization of the nonmagnetic VCSEL is negligible. The modulation of the output polarization Π_c with bias current was measured at different saturation magnetic fields, and the data are shown in Fig. 3(a). Again, the agreement with calculated results is very good. As the pump current reaches threshold, the carrier concentration of the polarized lasing mode with higher gain (say, S^+) becomes clamped at n_{th}. Further increase in pump current will increase the carrier concentration of the mode with lower gain (S^-), until n_{th} is reached for this mode also and the mode will lase. It is easily seen that the spin polarization in the QD active region will steadily decrease as the injection increases beyond the point where the first threshold (for S^+) is reached. This is also the overall threshold for the laser. Intuitively, it is expected that, in the injection regime between the thresholds for S^+ and S^-, the output polarization will steadily increase and then decrease after the threshold for S^- is crossed. However, considering the transport of injected spin-polarized carriers from the ferromagnetic contact to the active region by spin diffusion and the steady decrease of the spin polarization in the active (gain) region after the threshold of S^+ is reached, the pump spin polarization P_{spin} also decreases, as illustrated in Fig. 1(b). This leads to a decrease in output circular polarization as soon as the pump current increases beyond the threshold (for S^+). Thus the intuitive picture of the variation of output polarization would be valid only if diffusive transport of injected carriers is neglected and P_{spin} is held constant [inset in Fig. 3(a)]. This is the first demonstration of electrical modulation of the output polarization of a semiconductor laser. We define a modulation index as $\Delta\Pi_c/\Delta(I/I_{\text{th}})$, and this parameter is plotted in Fig. 3(b) as a function of normalized current along with the calculated data. The index goes through a maximum value of 0.6 at $I/I_{\text{th},0} \cong 1$ and decreases rapidly for high bias currents due to significant reduction of gain anisotropy in this range.

In conclusion, we have studied the effects of spin-induced gain anisotropy in spin-polarized lasers. Analytic expressions have been derived for threshold current reduction, output polarization, and the gain anisotropy parameter, taking into account the diffusion of spin-polarized carriers from the ferromagnetic contact to the active region and the spin-coupled laser rate equations. The validity of the derivations is endorsed by excellent agreement of calculated values of Π_c and $\Delta I_{\text{th}}(H)/I_{\text{th},0}$ with those obtained from measurements made with spin VCSELs having InAs/GaAs self-organized QDs as the gain media.

The authors acknowledge the support provided by the Office of Naval Research under Grant No. N00014-06-1-0025

*pkb@eecs.umich.edu

[1] C. J. Chang-Hasnain *et al.*, IEEE J. Quantum Electron. **27**, 1402 (1991).
[2] M. Shimuzi *et al.*, Electron. Lett. **27**, 1067 (1991).
[3] K. D. Choquette D. A. Richie, and R. E. Leibenguth, Appl. Phys. Lett. **64**, 2062 (1994).
[4] I. Sato *et al.*, Angew. Chem., Int. Ed. **40**, 1096 (2001).
[5] J. Rudolph *et al.*, Appl. Phys. Lett. **87**, 241117 (2005).
[6] M. Holub *et al.*, Phys. Rev. Lett. **98**, 146603 (2007).
[7] M. Holub and P. Bhattacharya, J. Phys. D **40**, R179 (2007).
[8] R. Fiederling *et al.*, Nature (London) **402**, 787 (1999).
[9] A. Greilich *et al.*, Science **313**, 341 (2006).
[10] *Optical Orientation*, edited by F. Meier and B. P. Zakharchenya (Elsevier Science, Amsterdam, 1984).
[11] M. I. D'yakonov and V. I. Perel', Fiz. Tverd. Tela **13**, 3581 (1971) [Sov. Phys. Solid State **13**, 3023 (1971)].
[12] Z. G. Yu and M. E. Flatté, Phys. Rev. B **66**, 201202 (2002).
[13] D. Basu *et al.*, Appl. Phys. Lett. **92**, 091119 (2008).
[14] R. P. Panguluri *et al.*, Phys. Rev. B **68**, 201307(R) (2003).
[15] D. Saha, M. Holub, P. Bhattacharya, and Y. C. Liao, Appl. Phys. Lett. **89**, 142504 (2006).
[16] M. San Miguel, Q. Feng, and J. V. Moloney, Phys. Rev. A **52**, 1728 (1995).
[17] See EPAPS Document No. E-PRLTAO-102-006912 for derivation of all the analytical expressions for a spin laser. For more information on EPAPS, see http://www.aip.org/pubservs/epaps.html.
[18] N. Kirstaedter *et al.*, Appl. Phys. Lett. **69**, 1226 (1996).
[19] S. Ghosh *et al.*, Appl. Phys. Lett. **79**, 722 (2001).
[20] Igor Žutić, Jaroslav Fabian, and S. Das Sarma, Rev. Mod. Phys. **76**, 323 (2004).
[21] R. Ram *et al.*, IEEE Photonics Technol. Lett. **8**, 599 (1996).
[22] A. T. Hanbicki *et al.*, Appl. Phys. Lett. **80**, 1240 (2002).
[23] E. I. Rashba, Phys. Rev. B **62**, R16 267 (2000).